

RESEARCH ARTICLE

10.1002/2014WR016577

Companion to *Tejedor et al.* [2015],
doi:10.1002/2014WR016604.

Special Section:

Connectivity, Non-Linearity,
and Regime Transitions in
Future Earthscapes

Key Points:

- Establish a quantitative framework for delta channel connectivity and dynamics
- Compute delta's steady fluxes, contributing and nourishment areas algebraically
- Construct vulnerability maps to identify hot spots of change

Correspondence to:

A. Tejedor,
alej.tejedor@gmail.com

Citation:

Tejedor, A., A. Longjas, I. Zaliapin, and E. Foufoula-Georgiou (2015), Delta channel networks: 1. A graph-theoretic approach for studying connectivity and steady state transport on deltaic surfaces, *Water Resour. Res.*, *51*, 3998–4018, doi:10.1002/2014WR016577.

Received 20 OCT 2014

Accepted 13 FEB 2015

Accepted article online 24 APR 2015

Published online 9 JUN 2015

Delta channel networks: 1. A graph-theoretic approach for studying connectivity and steady state transport on deltaic surfaces

Alejandro Tejedor¹, Anthony Longjas¹, Ilya Zaliapin², and Efi Foufoula-Georgiou^{1,3}

¹National Center for Earth-surface Dynamics and St. Anthony Falls Laboratory, University of Minnesota, Minneapolis, Minnesota, USA, ²Department of Mathematics and Statistics, University of Nevada, Reno, Nevada, USA, ³Department of Civil, Environmental and Geo- Engineering, University of Minnesota, Minneapolis, Minnesota, USA

Abstract River deltas are intricate landscapes with complex channel networks that self-organize to deliver water, sediment, and nutrients from the apex to the delta top and eventually to the coastal zone. The natural balance of material and energy fluxes, which maintains a stable hydrologic, geomorphologic, and ecological state of a river delta, is often disrupted by external perturbations causing topological and dynamical changes in the delta structure and function. A formal quantitative framework for studying delta channel network connectivity and transport dynamics and their response to change is lacking. Here we present such a framework based on spectral graph theory and demonstrate its value in computing delta's steady state fluxes and identifying upstream (contributing) and downstream (nourishment) areas and fluxes from any point in the network. We use this framework to construct vulnerability maps that quantify the relative change of sediment and water delivery to the shoreline outlets in response to possible perturbations in hundreds of upstream links. The framework is applied to the Wax Lake delta in the Louisiana coast of the U.S. and the Niger delta in West Africa. In a companion paper, we present a comprehensive suite of metrics that quantify topologic and dynamic complexity of delta channel networks and, via application to seven deltas in diverse environments, demonstrate their potential to reveal delta morphodynamics and relate to notions of vulnerability and robustness.

1. Introduction

Deltas are landforms with channels that deliver water, sediment, and nutrients from rivers to oceans or to inland water bodies via multiple pathways. These systems evolve naturally by maintaining the balance between subsidence due to compaction and new land formation due to sediment deposition from the river upstream. This dynamic interaction results in a low-relief terrain with slopes as low as 1.0×10^{-5} and intricate spatial patterns of channels and islands [e.g., *Wright and Coleman*, 1973; *Galloway*, 1975; *Saito et al.*, 2000; *Paola et al.*, 2011]. Deltas are home to more than half a billion people worldwide, highly productive regions supporting extensive agriculture, are rich in biodiversity and natural resources, and are ports of entry and economic hot spots. Yet, they are deteriorating at an alarming rate due to human (upstream and local exploration) and climate change (sea level rise) [*Syvitski*, 2008; *Blum and Roberts*, 2009; *Syvitski et al.*, 2009; *Vörösmarty et al.*, 2009; *Bucx et al.*, 2010; *Foufoula-Georgiou et al.*, 2013].

Any alteration in the delta network can provoke physical (channel morphology), biological (ecosystems), and socioeconomic changes. For example, dams and divergence structures built upstream to satisfy demands for water and energy reduce sediment and water delivery to the delta surface and to the coastline, thereby depriving delta growth and contributing to substantial reorganization of its channels and ecosystems [*Edmonds et al.*, 2010; *Ziv et al.*, 2012; *Filip and Giosan*, 2014]. Dikes, embankments, and sluice gates built on the delta surface to satisfy irrigation demands and flood control impose localized perturbations that disconnect rivers from their floodplains, drain wetlands, and alter vegetation with considerable consequences on fine sediment accretion and ecosystem functioning [e.g., *Rabalais et al.*, 2002; *Larsen et al.*, 2009]. Sea level rise causes saltwater intrusion, accelerates subsidence, and destructs vegetation close to the coast, and imposes ecogeomorphologic changes which propagate upstream [e.g., *Chen and Stanley*, 1998; *Nyman and DeLaune*, 1999; *Goodbred*, 2003; *Martin et al.*, 2009; *Anthony and Gratiot*, 2012].

Several recent studies have focused on modeling delta growth and evolution with simple radially averaged models [Parker *et al.*, 1998; Kim *et al.*, 2009a, 2009b], detailed hydrodynamic models [e.g., Edmonds and Slingerland, 2007], reduced complexity models [Seybold *et al.*, 2007, 2009; Liang *et al.*, 2015a, 2015b], and laboratory experiments (see Paola *et al.* [2009] for a review). Using such models for example, the effect of sediment flux and composition on the self-forming patterns of deltaic channels has been studied [Edmonds and Slingerland, 2010]. Also, relationships between surface area growth, shoreline length, channel hydraulic properties, and island shapes and sizes have been developed and attempts have been made to propose metrics that can differentiate between deltas [Jerolmack and Swenson, 2007; Martin *et al.*, 2009; Wolinsky *et al.*, 2010; Edmonds *et al.*, 2011; Geleynse *et al.*, 2012; Passalacqua *et al.*, 2013]. At the same time, formal methodologies for studying delta network topology and dynamic processes operating on them are still lacking. The pioneering work on the problem of quantifying delta channel network topology is attributed to Smart and Moruzzi [1971]. They proposed for the first time to abstract the channel network as a directed graph and use graph theory for its topological analysis. Although this work set the foundation for such an approach, the metrics proposed were very simple and were derived by “simple heuristic methods” [Smart and Moruzzi, 1971, p. 5] instead of formal graph-theoretic approaches, thereby limiting the range of metrics that could be considered. For example, the central topologic metric proposed in Smart and Moruzzi [1971] was the so-called recombination factor α , which is the ratio of the number of junctions (points where two channels combine to form one) to the number of forks (points where one channel divides into two). They also introduced the “connectivity matrix” (what will be defined formally herein in section 2.2 as the adjacency matrix which is the standard terminology in graph theory) and alluded to the fact that “all topologic properties of the network can be determined by simple manipulation of the matrix elements of the connectivity matrix” [Smart and Moruzzi, 1971, p. 9]. However, they limited the use of the connectivity matrix to deriving only one parameter: the total number of different paths from the source (apex) to the coast.

The purpose of our paper is to revive and formalize the use of spectral graph theory for the analysis of delta channel networks both in terms of their topologic structure and also in terms of their dynamic structure, i.e., partition of fluxes within the network. Specifically, we conceptualize a delta channel network as a graph and use its (weighted) Laplacian—a matrix summarizing the information about the node connections and their strengths—to answer various questions about the structure and dynamics of a delta network. An especially important role in this approach is played by the *eigenvalues* and *eigenvectors* of the graph Laplacian. The collection of all Laplacian eigenvalues is called the *spectrum*, and the branch of mathematics that studies graphs via the eigenvalues and eigenvectors of a graph Laplacian is called *spectral graph theory*. This is a well-established and rapidly growing field in view of the ubiquitous presence of networks in natural and engineered systems, e.g., food webs, transportation networks, ecosystems, the World Wide Web, and social networks, to name but a few [e.g., Chung, 1997; Barrat *et al.*, 2008]. Our study uses the recent results from the spectral theory of directed graphs [Agaev and Chebotarev, 2005; Caughman and Veerman, 2006] that offer a useful interpretation of the null-space (space spanned by the eigenvectors of zero eigenvalue) of the Laplacian and have an immediate application to the analysis of deltaic systems. Specifically, we use this theory to identify subnetworks in the delta system, such as upstream (contributing) and downstream (nourishing) subnetworks for any node in the delta.

To study transport dynamics on a delta network, we adopt here a “package of flux” point of view. Namely, we consider a conceptual individual package of flux (of sediment, water, or nutrients) that enters the system at the apex and propagates downstream until it arrives at a channel junction. Here it randomly decides which of possible further paths to take, with the probability of taking a particular path depending on the channel width or any other suitable characteristic. In other words, the package performs a *random directed walk* along the network of delta channels. A flow in the delta is conceptualized by a large number of noninteracting flux packages that independently perform such a random downstream walk. This representation allows us to use the well-developed tools from the random processes theory. For instance, a steady flux through the delta corresponds to the stationary distribution of the above random walk and can be derived by using operations on the Laplacian matrix.

The paper is organized as follows. Section 2 reviews the graph-theoretic concepts leading to the directed weighted graph Laplacian, its spectrum, and null-space. Section 3 addresses the problems of representing a delta as a directed graph, finding the steady flux through the delta, and identifying the contributing and

nourishment subnetworks for a given node. Application of the framework to two river deltas, the Wax Lake (U.S.) and Niger (West Africa), is presented in section 4. Quantification of delta vulnerability using this approach is discussed in section 5. Section 6 presents conclusions and gives a prelude to the companion paper where spectral analysis and entropy-based approaches are used to construct a suite of metrics depicting the topologic and dynamic connectivity of deltas and their subnetworks and analyze how these relate to robustness and vulnerability.

2. Directed Graphs: A Brief Review

A network is any system that admits an abstract mathematical representation as a graph whose nodes (vertices) identify the elements of the system and in which the set of connecting links (edges) represent the presence of a relation or interaction among those elements [Newman, 2003; Barrat et al., 2008]. Networks provide a theoretical framework that allows a convenient representation of interrelations in complex systems by mapping interactions among a large number of individual components and studying their feedbacks and dynamics. Such network-type representations of complex systems are common in ecology, population dynamics, plant physiology, food webs, epidemiology, social sciences, and transportation (see Newman [2003] for an extensive review and references).

In geomorphology, tributary river networks (networks that distribute their fluxes from several upstream nodes to a single downstream outlet via convergent pathways) have been studied extensively both in terms of their topologic structure and their dynamics [e.g., see Rodriguez-Iturbe and Rinaldo, 1997, and references therein]. However, the structure and dynamics of distributary river networks (networks that deliver their fluxes from a single upstream node to one or several downstream nodes via convergent and divergent pathways) is still not as well developed with the exception of some work on tidal networks [e.g., Fagherazzi et al., 1999; Rinaldo et al., 1999a, 1999b] and braided river networks [e.g., Sapozhnikov and Foufoula-Georgiou, 1996, 1997, 1999]. The present work seeks to advance the quantitative representation of distributary networks and specifically to provide formalisms by which such networks can be studied both for their static topology and dynamic transport of fluxes, including the propagation of disturbances and alterations from one part of the system to the rest.

The proposed approach relies on studying networks via graph-theoretic methods. Graph theory for the study of networks has a long history going back to Euler [1736] in solving the Konigsberg bridges problem. In particular, spectral graph theory studies the properties of graphs via the eigenvalues and eigenvectors of their associated graph matrices: the adjacency matrix (A) and the Laplacian matrix (L). These matrices allow a natural link between a discrete representation (such as graphs) and a continuous representation (such as vector spaces) and transform many problems of interest to linear algebraic problems that can be solved by matrix manipulations. A review of the essential elements of this theory is presented below, and the reader is referred to Newman [2003, 2010] and Barrat et al. [2008] for comprehensive reviews.

2.1. Edge Direction, Cycles, and Roots

A graph $G = (\mathcal{V}, \mathcal{E})$ is a collection of vertices $\mathcal{V} = \{v_i, i = 1, \dots, N$, and edges $\mathcal{E} = \{(uv)\}, u, v \in \mathcal{V}$, with the notation (uv) signifying that the edge connects the vertices u and v . We will consider only *simple* graphs that have at most one edge between any two vertices. We also prohibit *self-loops*, which are edges of the form (uu) . A graph is called *directed*, or digraph, if its edges have directions, so the edge pairs (uv) are ordered. A digraph is called *acyclic* if there are no directed paths from a vertex to itself. An acyclic digraph imposes well-defined parent-child relationships among the vertices. Specifically, each edge (vu) connects a *parent* v to a *child* (offspring) u . In general, each vertex may have multiple offspring and parents. The vertices with no offspring are called *leaves*. A digraph is called *rooted* if there is a vertex r such that there exists a directed path from r to any other vertex in the graph.

This terminology suggests that there exist four types of directed graphs, defined by presence/absence of cycles and roots. Figure 1 illustrates different types of graphs. Figure 1a shows an undirected graph with four vertices A, B, C, D, and four undirected edges (AB), (AC), (AD), and (CD). Figures 1b–1e illustrate the four types of digraphs. Figure 1b shows a digraph with no root and no cycles. To verify the absence of roots, we observe that A is not connected to D and B; B is not connected to D; C is not connected to any of the other vertices; and D is not connected to B. Figure 1c shows a digraph with a single root A and no cycles. Figure

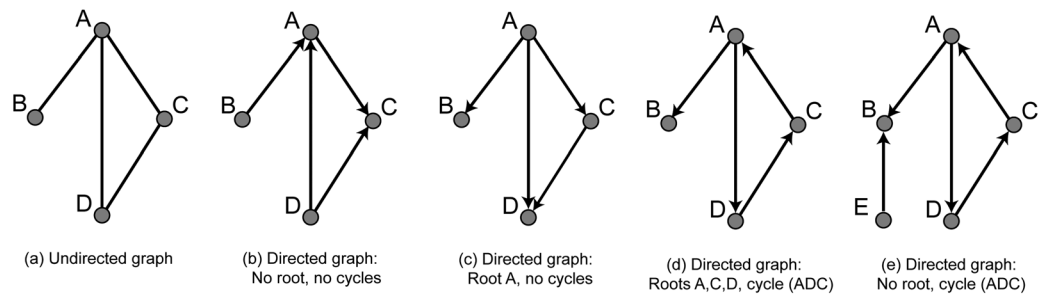


Figure 1. Examples of graphs. (a) Undirected graph; (b) directed graph (digraph) with no root and no cycles; (c) digraph with root A and no cycles (rooted acyclic digraph of interest in this study); (d) digraph with roots A, C, D, and cycle (ADC); (e) digraph with no root and cycle (ADC).

1d shows a digraph with roots A, C, D, and cycle (A → D → C → A) = (ADC). Figure 1e shows a digraph with no root and cycle (ADC). The absence of roots is verified by observing that E is not connected to A, C, D, and none of the vertices is connected to E. As will be seen in the sequel, rooted acyclic digraphs play an important role in this study as they are well suited to describe propagation of fluxes along a deltaic network from the sources (roots) to the outlets in the unique downstream direction, which prevents forming flow cycles.

2.2. Adjacency Matrix

A digraph G can be uniquely specified by its square $N \times N$ asymmetric adjacency matrix $A(G) = \{a_{uv}\}_{1 \leq u, v \leq N}$ with elements given by

$$a_{uv} = \begin{cases} 1, & \text{if there exists edge } (vu) \\ 0, & \text{otherwise} \end{cases} \quad (1)$$

Notice that, according to this definition, a directed edge from vertex 1 to vertex 2 corresponds to a nonzero element (2,1), and not (1,2), of the adjacency matrix A , which is illustrated in Figure 2. This standard convention proves useful for many matrix operations on graphs.

The adjacency matrix conveniently summarizes the information about the number of parents and offspring for every vertex in a graph. Namely, the number d_u^{in} of parents for vertex u (number of edges arriving at vertex u) is the sum of the elements in the u th row of A ; it is called the *in-degree* of u . The number d_u^{out} of offspring for vertex u (number of edges leaving vertex u) is the sum of the elements of the u th column of A ; it is called the *out-degree* of u . In matrix notations, the in-degree of u is the u th element of the vector

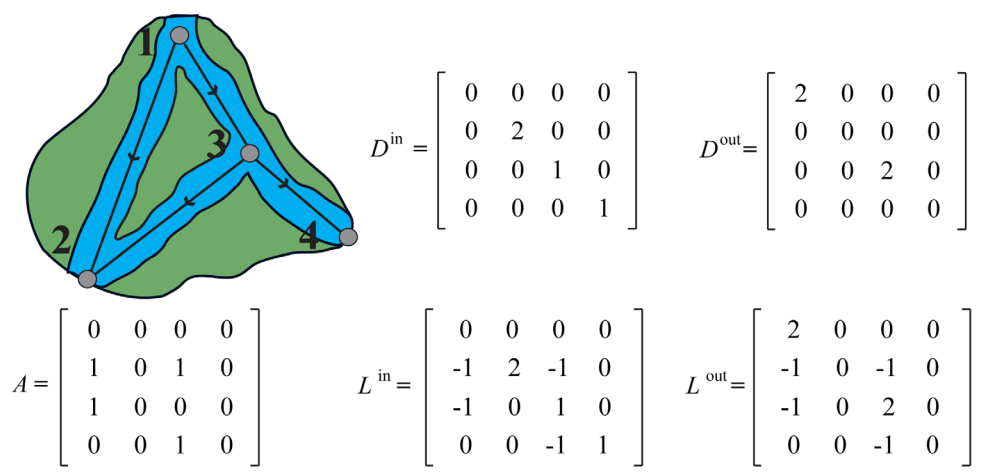


Figure 2. Adjacency, degree, and Laplacian matrices of a digraph: an example. The figure shows the matrices A , D^{in} , D^{out} , L^{in} , and L^{out} for the rooted acyclic digraph with four vertices and four edges shown in the top left corner.

$$A\mathbf{1} = \left[\sum_{i=1}^N a_{1i}, \dots, \sum_{i=1}^N a_{Ni} \right]^T \equiv [d_1^{\text{in}}, \dots, d_N^{\text{in}}]^T, \quad (2)$$

and the out-degree is the u th element of the vector

$$A^T\mathbf{1} = \left[\sum_{i=1}^N a_{i1}, \dots, \sum_{i=1}^N a_{iN} \right]^T \equiv [d_1^{\text{out}}, \dots, d_N^{\text{out}}]^T, \quad (3)$$

where $\mathbf{1}$ is the $N \times 1$ vector-column with all elements equal to 1, and A^T denotes the transpose of A .

In the same fashion, it is easy to show that the u th element of the vector $A^k\mathbf{1}$ is the number of distinct paths that can be constructed by moving exactly k steps along the directed edges of G starting from u . This number can differ from the number of offspring at distance k from u , since different paths may lead to the same offspring vertex. Similarly, the u th element of the vector $(A^T)^k\mathbf{1}$ is the number of distinct paths that can be constructed by moving exactly k steps along the edges of G in the *reverse* direction starting from u .

Sometimes, the edges of a graph are given weights w_{uv} ; these weights could represent the strength of the relationship between nodes u and v . In this case, the graph is specified by its *weighted* adjacency matrix W with nonzero elements w_{uv} . In the delta networks, the weights could correspond to the channel widths, and thus determine the partition of flux at each node among its downstream nodes, and hence determine the flux distribution in the whole network. In general, in a *marked* graph $G = (\mathcal{V}, \mathcal{E}, F)$, each vertex u has a quantitative (and possibly multidimensional) characteristic F_u .

Finally, for a graph $G = (\mathcal{V}, \mathcal{E})$, we can construct a new graph $G^R = (\mathcal{V}, \mathcal{E}^R)$ which is the graph on the same set of vertices \mathcal{V} and with the same set of edges but with *reverse* directions—that is, $(uv) \in \mathcal{E}^R$ if and only if $(vu) \in \mathcal{E}$. We call G^R the graph *reverse* to G ; it is used in this study to identify the upstream networks (upstream contributing areas) that contribute to a given node in the delta.

2.3. Directed Weighted Graph Laplacian

Exploration of graph properties is facilitated by considering the so-called *directed graph Laplacian* L , which may take two alternative forms for a digraph G :

$$L^{\text{in}}(G) = D^{\text{in}}(G) - A(G) \quad \text{or} \quad L^{\text{out}}(G) = D^{\text{out}}(G) - A(G), \quad (4)$$

where D^{in} (D^{out}) is the in-degree (out-degree) matrix for G defined as the $N \times N$ diagonal matrix with diagonal elements taken from $A\mathbf{1}$ ($A^T\mathbf{1}$):

$$D^{\text{in}} = \begin{bmatrix} d_1^{\text{in}} & 0 & \dots & 0 \\ 0 & d_2^{\text{in}} & \dots & 0 \\ \vdots & \vdots & \ddots & \vdots \\ 0 & 0 & \dots & d_N^{\text{in}} \end{bmatrix}, \quad D^{\text{out}} = \begin{bmatrix} d_1^{\text{out}} & 0 & \dots & 0 \\ 0 & d_2^{\text{out}} & \dots & 0 \\ \vdots & \vdots & \ddots & \vdots \\ 0 & 0 & \dots & d_N^{\text{out}} \end{bmatrix}. \quad (5)$$

Figure 2 shows an example of degree matrices and respective Laplacians for a simple digraph on four vertices.

We observe the following relations between matrix characteristics of graph G and the reverse graph G^R :

$$D^{\text{in}}(G) = D^{\text{out}}(G^R), \quad D^{\text{out}}(G) = D^{\text{in}}(G^R), \quad A(G) = A(G^R)^T,$$

which imply

$$L^{\text{in}}(G) = [L^{\text{out}}(G^R)]^T, \quad L^{\text{out}}(G) = [L^{\text{in}}(G^R)]^T.$$

The graph Laplacian can be also defined using a weighted adjacency matrix:

$$L_W^{\text{in,out}}(G) = D_W^{\text{in,out}}(G) - W(G), \quad (6)$$

with

$$D_W^{in} = \begin{bmatrix} \sum_{i=1}^N W_{1i} & 0 & \dots & 0 \\ 0 & \sum_{i=1}^N W_{2i} & \dots & 0 \\ \vdots & \vdots & \ddots & \vdots \\ 0 & 0 & \dots & \sum_{i=1}^N W_{Ni} \end{bmatrix}, \quad D_W^{out} = \begin{bmatrix} \sum_{i=1}^N W_{i1} & 0 & \dots & 0 \\ 0 & \sum_{i=1}^N W_{i2} & \dots & 0 \\ \vdots & \vdots & \ddots & \vdots \\ 0 & 0 & \dots & \sum_{i=1}^N W_{iN} \end{bmatrix}. \quad (7)$$

2.4. Why Do We Call It Laplacian?

To provide intuition behind the name *Laplacian*, recall that the continuous Laplace operator Δ is defined as the divergence of the gradient of a sufficiently smooth function $f(x_1, \dots, x_n)$:

$$\Delta f = \nabla^2 f = \nabla \cdot \nabla f = \sum_{i=1}^n \frac{\partial^2 f}{\partial x_i^2}. \quad (8)$$

For a scalar function $f(x)$, this becomes $\Delta f = \frac{d^2 f}{dx^2}$, which is simply the second derivative. For a time series $f(x)$ observed at the discrete grid $x = 0, \pm 1, \pm 2, \dots$, the gradient (first derivative) can be approximated by taking the convolution of f with the two-element kernel $d_1 = [-1 \ 1]$. In this case, the Laplace operator (second derivative) is approximated by the convolution of f with $d_2 = d_1 * d_1 = [1 \ -2 \ 1]$. In plain language, this is the sum of the values of f at the two immediate neighbors of the location x minus twice the value at x : $f(x - 1) - 2f(x) + f(x + 1)$. The same logic can be applied in higher dimensions: if the gradient is approximated by the difference between the values of f at two neighbor points in a given direction, then the Laplacian at point x is the sum of the immediate neighboring values minus the value at x multiplied by the number of its neighbors ($2k$ in a k -dimensional system). This general principle applied to a directed graph leads to the discrete Laplace operator of equation (4).

As we mention in section 1, the graph Laplacian plays a key role in studying diffusion and random walks on graphs, network connectivity, graph partitioning, and many other problems [Newman, 2010]. This study will rely heavily on the properties of the *null-space* of the graph Laplacian discussed in the next section.

2.5. Null-Space of the Digraph Laplacian

Consider a digraph Laplacian $L = L^{in}$ (either weighted or unweighted) of size $N \times N$. An *eigenvector* $x = [x_1, \dots, x_N]^T$ of L is a real vector such that its right multiplication by L is equivalent to scaling by a constant λ :

$$Lx = \lambda x. \quad (9)$$

The scaling constant λ that solves the equation (9) is called the *eigenvalue* corresponding to x . The set of the eigenvalues $\lambda_0 \leq \lambda_1 \leq \dots \leq \lambda_{N-1}$, some of which might be repeating, is called the *spectrum* of L . The characterization of the digraph Laplacian spectrum can be found in Bauer [2012]. Here we are interested only in a particular eigenvalue $\lambda = 0$.

It readily follows from the definition of the Laplacian that $\lambda = 0$ always belongs to the spectrum of L and corresponds to the all-ones eigenvector $x = [1, \dots, 1]^T$. If the multiplicity of $\lambda = 0$ is larger than 1, that is, if there exist several linearly independent vectors that solve $Lx = 0$, then the corresponding eigenvectors are not unique. Those vectors form a basis (not necessarily orthogonal) in the *null-space* of L :

$$\text{null}(L) = \{x : Lx = 0\}.$$

We show in this paper that the null-space of L plays an important role in describing the essential topologic and transport properties of a digraph.

3. Graph Analysis of Deltas: Computation of Fluxes and Subnetworks

This section introduces a graph representation of a delta system of channels, describes the process of identifying delta subnetworks, and computes channel fluxes via the graph spectral representation.

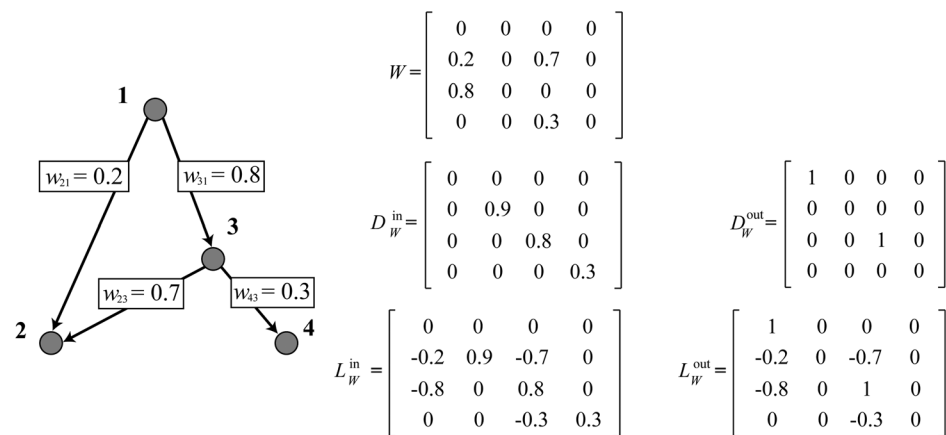


Figure 3. (left) Rooted acyclic digraph with a weighted adjacency matrix W . The figure shows the adjacency matrix W , the corresponding degree matrices $D_W^{\text{in}}, D_W^{\text{out}}$, and the Laplacians $L_W^{\text{in}}, L_W^{\text{out}}$ for the digraph. The weights w_{ij} are shown next to the graph edges and capture the partitioning of flux at each channel bifurcation.

3.1. Graph Representation of a Delta System

We consider all the links in the delta network that connect the apex to the shoreline outlets, and assume a unique downstream direction of fluxes along the delta channels. We note that in real deltas this might not always be the case as many channels might be bidirectional, especially tidal channels close to the coast. Such cases cannot be handled by the framework presented herein but suitable extensions might be possible in the future.

The topological arrangement of the delta channels can be represented by a marked rooted acyclic directed graph G . The delta apex corresponds to the root of G ; the shoreline outlets are represented by the leaves; the physical points where channels intersect (combine or split) or terminate are depicted by vertices; and the channel segments between intersections/splits/outlets correspond to edges. The direction of flux through the delta (from root to outlets) is represented by the edge directions. The flux intensity at node i is given by time-dependent mark $F_i(t)$. The distribution of the flux at a parent vertex v among the offspring vertices (x, \dots, z) is given by vector (w_{xv}, \dots, w_{zv}) such that $w_{xv} + \dots + w_{zv} = 1$ guaranteeing preservation of flux at bifurcating channels. The weights w_{uv} form the weighted adjacency matrix W .

Figure 3 shows an example of a weighted digraph that represents a simple delta system with a single apex (vertex 1), two outlets (vertices 2 and 4), and nonuniform distribution of the parental flux among the offspring. The figure shows the weighted adjacency matrix W as well as the corresponding in/out-degree matrices $D_W^{\text{in}}, D_W^{\text{out}}$ and the respective Laplacians $L_W^{\text{in}}, L_W^{\text{out}}$. This example will be used below to illustrate the graph-based analysis of delta transport.

3.2. Steady Flow

At steady state, the flow F_i through vertex i equals the total inflow from its parents: $F_i = \sum_{j=1}^N w_{ij} F_j$. The summation here is taken over all vertices j , although the weights w_{ij} have nonzero values only for the parents of vertex i . This equation applies to all the vertices i except the root (which does not have an upstream node) and leaves (which do not have offspring)—at these vertices the flux cannot reach a nontrivial steady state. From the package-of-flux perspective outlined in section 1, a package that reaches an outlet will sit there forever. Hence, the only possible stationary distribution of a random walk on our graph is one concentrated at the outlets, which does not lead to any meaningful conclusions. To avoid this problem, we consider a *cycled* version of the network, where the outlets (leaves) directly drain their entire flux to the apex (root). The weighted adjacency matrix for this new network is denoted by \tilde{W} . Now we seek a steady state solution $F = (F_1, \dots, F_N)^T$ of the system

$$F_i = \sum_j \tilde{w}_{ij} F_j, \quad i = 1, \dots, N. \quad (10)$$

This can be written in matrix notation as $F = \tilde{W} F$ (the steady flux distribution F is invariant to the action of \tilde{W}), or $(I_N - \tilde{W})F = \mathbf{0}_N$, where I_N is the $N \times N$ identity matrix, and $\mathbf{0}_N$ is the $N \times 1$ vector of zeros. In other

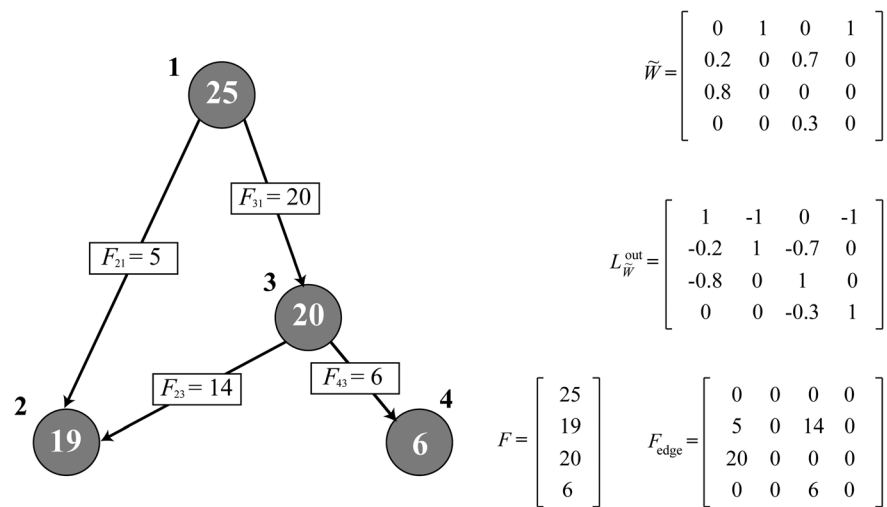


Figure 4. Computation of steady flow through the digraph of Figure 3. The input flux at the root is 25 units (fluxes indicated by circled numbers at nodes). The figure shows the cycled weighted adjacency matrix \tilde{W} , the corresponding weighted out-degree Laplacian $L_{\tilde{W}}^{\text{out}}$, the steady flow solution F at the vertices, and the steady flow F_{edge} at the edges. Notice the difference of \tilde{W} from the weighted adjacency matrix W of Figure 3; the top row in \tilde{W} reflects the cycling of the flux from nodes 2 and 4 back to 1 for mass balance in obtaining the steady state solution. The node fluxes F_i have been obtained from the solution of $L_{\tilde{W}}^{\text{out}} F = 0$ (the eigenvector that spans the null-space of $L_{\tilde{W}}^{\text{out}}$) while the steady state fluxes F_{uv} at the edges have been obtained as $F_{uv} = W_{uv} F_v$ (see text).

words, we need to identify the null-space of the matrix $(I_N - \tilde{W})$. We notice that I_N is the out-degree matrix for \tilde{W} , so $(I_N - \tilde{W})$ is in fact the out-degree graph Laplacian for the weighted adjacency matrix \tilde{W} . It is clear from the flux interpretation that there exists a unique solution to this problem. We summarize these observations below.

Consider a delta channel network represented by a rooted acyclic digraph G with weighted cycled adjacency matrix \tilde{W} . The steady flow $F = (F_1, \dots, F_N)^T$ at the vertices is given (up to a scalar factor) by the eigenvector that spans the null-space of the out-degree graph Laplacian $L_{\tilde{W}}^{\text{out}} = I_N - \tilde{W}$, i.e., F is the solution of $L_{\tilde{W}}^{\text{out}} F = 0$. Accordingly, the steady flow at an edge (vu) is given by $F_{uv} = F_v W_{uv}$.

Figure 4 illustrates this result in the simple weighted digraph of Figure 3. One can check that the eigenvector F computed as presented above gives the consistent (and intuitively clear) flow values at the vertices and edges of the examined graph.

3.3. Contributing Subnetworks

Here we identify the *contributing subnetwork* R_u —the subnetwork that participates in draining fluxes from the apex to a given vertex u . We define the *exclusive part* H_u of a subnetwork R_u as the set of all vertices in R_u that drain exclusively to the outlet u . The *common part* C_u of a subnetwork R_u is defined as the complement of H_u in R_u , that is as the set of all the vertices that drain to at least one other outlet besides u . *Caughtman and Veerman* [2006] established the existence of a particularly useful basis in the null-space of the weighted graph Laplacian, which offers an elegant solution to the problem of identifying R_u , H_u , C_u and determining the steady state flux distribution within R_u .

We start below with identifying the contributing subnetworks that drain the apex to the delta outlets (shoreline nodes) and then extend this theory to identifying contributing subnetworks that drain the apex to any downstream node of interest.

Consider a delta system represented by an acyclic graph G with a weighted adjacency matrix W . Assume that the system has k outlets indexed as $i = 1, \dots, k$. Then,

1. The null-space of the weighted in-degree Laplacian $L_W^{\text{in}}(G^R)$ for the reverse graph G^R has dimension (multiplicity of the eigenvalue zero) equal to the number of outlets k .
2. There exists a unique basis $\gamma_i, i = 1, \dots, k$, of this null-space in \mathbb{R}^N (i.e., the basis consists of k vectors each having N components) with the property

$$\gamma_i(j) = \delta_{ij} = \begin{cases} 1, & i=j, \\ 0, & i \neq j \end{cases} \text{ for } j=1, \dots, k.$$

That is, the component of the vector γ_i is unity at the outlet i ($\gamma_i(i) = 1$) and zero at all other outlets ($\gamma_i(j) = 0$ for $j \neq i, j = 1, \dots, k$).

3. The nonoutlet vertex v belongs to the contributing subnetwork R_i if and only if $\gamma_i(v) \neq 0$.
4. The vertex v belongs to the exclusive part H_i of the subnetwork R_i if and only if $\gamma_i(v) = 1$; the vertex v belongs to the common part C_i of the subnetwork R_i if and only if $0 < \gamma_i(v) < 1$.
5. If element w_{uv} of the weighted adjacency matrix W represents the proportion of flux at parental vertex v that drains to offspring vertex u , then the value $\gamma_i(v)$ equals the proportion of flux at vertex v that drains to the outlet i .

We observe that the structure of the contributing network is a topologic (rather than dynamic) property, which means that it should be independent of a particular physical meaning of the elements of W . This implies that the above results (1)–(4) stay true for *any* weight distribution within the adjacency matrix of G . For instance, the results are true for the unweighted adjacency matrix A .

The statements (1)–(4) above are a paraphrase of the original theorem proven in *Caughman and Veerman* [2006, theorem 3.3]. To demonstrate the additional property (5), consider a flow along the directed edges of G with the distribution of the parental flux among the offspring given by a weighted adjacency matrix $W = \{w_{vu}\}$ such that $w_{1u} + \dots + w_{Nu} = 1$ for any $u = 1, \dots, N$. The statement (5) is trivial for the outlets of G , which always belong to the exclusive part of their respective subnetworks, and hence considered to drain the entire flux to their own contributing subnetwork: $\gamma_i(i) = 1$. To prove the statement for the rest of the vertices, observe that by definition of the eigenvector

$$L_W^{\text{in}}(G^R)\gamma_i = [D_W^{\text{in}}(G^R) - W(G^R)]\gamma_i = [D_W^{\text{out}}(G) - W(G)^T]\gamma_i = 0,$$

which implies

$$D^{\text{out}}(G)\gamma_i = W(G)^T\gamma_i.$$

We notice that $D^{\text{out}}(G)\gamma_i(v) = \gamma_i(v)$ for all nonoutlet vertices v , because of our assumptions about the elements of $W(G)$. This means that the nonoutlet element v of the eigenvector γ_i equals the weighted average of its parental elements in G^R (or offspring elements in G):

$$\gamma_i(v) = \sum_{j=1}^N w_{vj}\gamma_i(j), \quad i=1, \dots, N.$$

The induction with the base at the leaves and steps along the directed edges of G^R completes the proof.

The result above is readily extended to identifying the subnetwork that drains fluxes from the apex to any chosen vertex, not necessarily an outlet. For that, one needs to make the examined vertex an outlet by disconnecting it from its offspring. The respectively modified weighted adjacency matrix is then used to obtain the result.

We notice that while the result of *Caughman and Veerman* [2006] guarantees the existence of a “good” basis γ_i in the null-space, one cannot be sure that exactly this basis will be found by a particular numerical method (software). However, this basis can be readily constructed from any alternative one using its characteristic property (2).

We illustrate the identification of contributing subnetworks in the simple digraph of Figure 5 (also used in Figures 3 and 4, above). The graph has two outlets (nodes 2 and 4). Accordingly, the multiplicity of the zero eigenvalue is two and the corresponding eigenvectors γ_2 and γ_4 describe the structure of the subnetworks contributing to the outlets. The subnetwork R_2 that contributes to the outlet {2} consists of vertices {1,2,3}; the subnetwork R_4 that contributes to the outlet {4} consists of the vertices {1,3,4}. Both the apex {1} and internal vertex {3} belong to the common part of both the subnetworks; and the outlets are the only exclusive parts of the respective subnetworks. The proportion of the flux that drains from each vertex to each

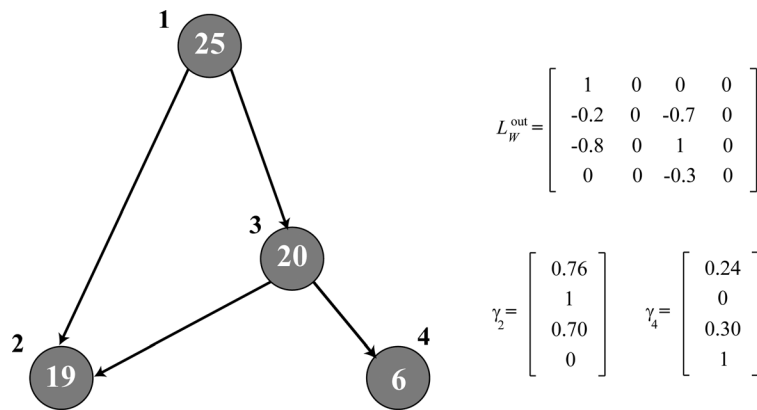


Figure 5. Contributing subnetworks for the outlets of the digraph of Figure 3. Here there are two contributing subnetworks draining the root (node 1) to the outlet nodes 2 and 4. The figure shows the weighted out-degree Laplacian $L_W^{\text{out}}(G) = L_W^{\text{in}}(G^R)^T$. The contributing subnetworks are constructed using the two eigenvectors γ_2 and γ_4 that span the Laplacian null-space, i.e., are the solutions of $L_W^{\text{out}}(G^R)\gamma = 0$. The eigenvector element $\gamma_i(v)$ shows the proportion of the flux at vertex v that drains to outlet i . For instance, $\gamma_2(1) = 0.76 = 19/25$ of the flux at vertex 1 drains to outlet 2, etc. See Figure 3 for the graph adjacency matrix and Figure 4 for the steady flow solution.

subnetwork is given by the eigenvectors γ_2 and γ_4 as indicated in the figure. It is easy to check that this solution is consistent with the steady flow values shown at the graph vertices.

3.4. Nourishing Subnetworks

In this section, we identify the nourishing subnetwork N_u —the subnetwork that drains fluxes from u to the outlets [Edmonds et al., 2011]. This is done by applying the same technique as above to the directed graph G rather than the reverse graph G^R . Namely, to identify the nourishing network for a node u , we first make u an apex by disconnecting it from the parents. The identification is then done using the following result, which is again a paraphrase of the original theorem by Caughman and Veerman [2006, theorem 3.3].

Consider a delta system represented by an acyclic digraph G . Assume that the system has k roots indexed as $i = 1, \dots, k$. Assume that the element w_{uv} of the weighted adjacency matrix W represents the proportion of flux at parental vertex v that drains to offspring vertex u . Then,

1. The null-space of the weighted in-degree Laplacian $L_W^{\text{in}}(G)$ has dimension (the multiplicity of the zero eigenvalue) equal to the number of roots k .
2. There exists a unique basis $\gamma_i(j)$, $i = 1, \dots, k$, of the null-space in \mathbb{R}^N (i.e., the basis has k vectors each having N components) such that

$$\gamma_i(j) = \delta_{ij} = \begin{cases} 1, & i=j; \\ 0, & i \neq j \end{cases} \quad \text{for } j=1, \dots, k$$

That is, the component of the vector γ_i is unity at the root i ($\gamma_i(i) = 1$) and zero at all other roots ($\gamma_i(j) = 0$ for $j \neq i, j = 1, \dots, k$).

3. The vertex v belongs to the nourishing subnetwork N_i of root i if and only if $\gamma_i(v) \neq 0$.

Figure 6 illustrates this result in the digraph of Figures 3–5. In this simple situation ($k = 1$), all the vertices belong to the nourishment subnetwork of the apex {1}.

4. Application to Two Real Deltas

In this study, we apply the graph Laplacian framework to the analysis of the Wax Lake and Niger deltas.

4.1. Wax Lake Delta

The Wax Lake delta is a relatively young river-dominated delta with a radial shoreline propagation (Figure 7, left). It receives input from the Mississippi River through the Atchafalaya River and the Wax Lake outlet consisting of an average discharge of 2900 m³/s and 2.35×10^7 tons yr⁻¹ of sediment [Roberts et al., 2003].

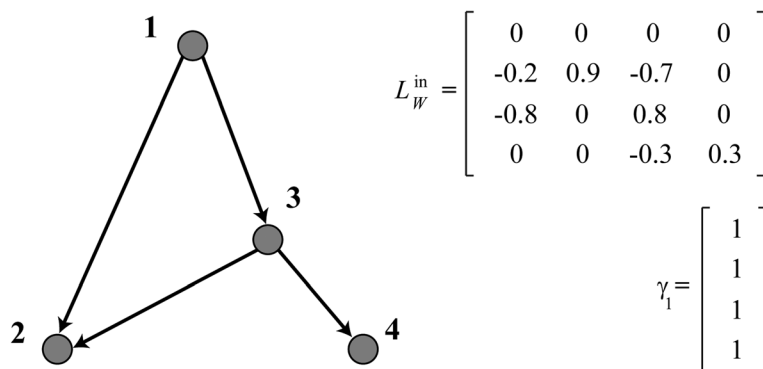


Figure 6. Nourishing subnetworks for the apex of the digraph of Figure 3. The figure shows the weighted in-degree Laplacian L_W^{in} and the single eigenvectors γ_1 that spans the Laplacian null-space, i.e., is the solution of $L_W^{in}(G)\gamma_1=0$. The eigenvector element $\gamma_1(v)$ is not equal to zero if and only if the vertex v receives fluxes from the apex. Since all vertices receive fluxes from the apex 1 in this example, hence the eigenvector has all elements equal to 1. See Figure 3 for the graph adjacency matrix.

Subaerial land began to emerge after the 1973 flood, and since then the delta has evolved with minimum human alteration [Roberts *et al.*, 1980]. In the last two decades, the delta surface has doubled to more than 100 km² from 52.1 km² in 1994 [Roberts *et al.*, 1997; Paola *et al.*, 2011]. Core data analysis reveals that sand accounts for two-thirds (67%) of the sediment deposits in the Wax Lake Delta [Roberts *et al.*, 1997]. Erosion occurs on the channel banks resulting in a median increase of 11% in channel widths since the early 1990s and island migration farther downstream [Shaw *et al.*, 2013]. We utilized the outline of the Wax Lake delta structure processed by Edmonds *et al.* [2011] and identified 59 links and 24 shoreline outlets. In our analysis, we only consider primary channels, which are links that provide direct paths from the delta apex to a shoreline outlet. The partition of the flow at a parental vertex among the immediate downstream channels is proportional to the channel width [Bolla Pittaluga *et al.*, 2003; Edmonds *et al.*, 2011].

4.2. Niger Delta

The Niger delta is an older, highly complex distributary network that has numerous loops and other intricate structures (Figure 7, right). The delta is very flat, with a gradient of 7×10^{-5} [Syvitski *et al.*, 2005]. The origin of the delta is estimated to be 80 million years ago during the Late Cretaceous [Short and Staeuble, 2004; Goudie, 2005]. Sediment in the delta is dominated by Quaternary sand, clay, and gravel [Reijers, 2011]. The Niger delta is fed by the Niger River, which delivers a mean annual water discharge of 6130 m³/s and 3.97×10^7 tons yr⁻¹ sediment discharge to the delta head [Syvitski *et al.*, 2005]. Unlike the Wax Lake delta, the Niger delta is classified as in peril mainly because of reduced water and sediment fluxes due to hundreds of dams and reservoirs upstream and accelerated compaction within the delta driven by oil and gas extraction. Increased tidal influence due to sea level rise is also causing saltwater intrusion that is affecting the floodplain ecology and threatening potable water supply in the region [Abam, 2001; Kuenzer *et al.*, 2014]. We consider the channel network outlined by Smart and Moruzzi [1971], consisting of 181 links that connect the Niger River to 15 shoreline outlets. Our study area is confined between the coordinates (5°22'18.51"N, 5°19'15.53"E) and (4°20'42.58"N, 6°42'44.74"E). Recent assessment of the Niger delta coastline using satellite imagery shows that in coastal areas where changes have been observed, erosion is more prevalent than sediment deposition [Adegoke *et al.*, 2010; Kuenzer *et al.*, 2014]. A comparison of the Smart and Moruzzi [1971] network with recent satellite images from the USGS Earth Explorer web site shows changes in the shoreline links since 1971, but the overall connectivity structure (primary channels) is still maintained. Water discharge is again assumed to be proportional to channel widths measured on Landsat images.

4.3. Steady Flux and Contributing, Nourishment Subnetworks

The steady state flux for the Wax Lake delta is illustrated in Figure 8a. There exists no dominant shoreline outlet for this delta—the maximum outlet flow of about 12% of the apex flux is achieved at 4 out of 24 outlets. We also observe that 25% (6 out of 24) of outlet links receive 60% of the flux at the apex. This result is comparable to the synthetic sediment flux distribution at the shoreline for the Wax Lake delta obtained by Edmonds *et al.* [2011]. The steady state flux for the Niger delta is illustrated in Figure 8c, where only five (out

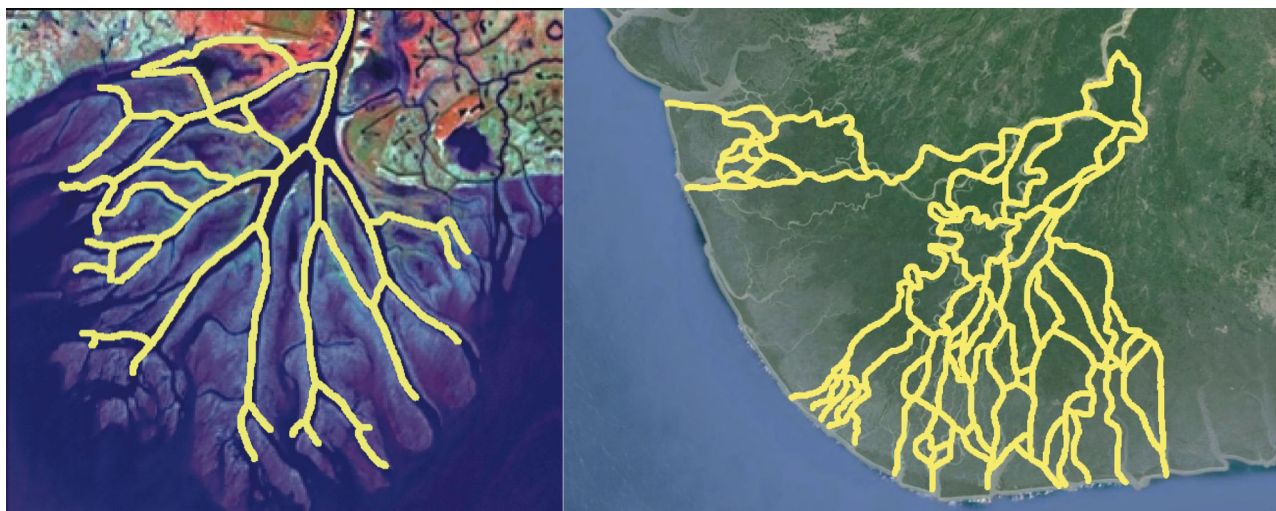


Figure 7. (left) Wax Lake delta in the Louisiana coast. The skeleton network (yellow lines) is superimposed on the aerial view of the delta (photo obtained in 2005 by the National Center of Earth-surface Dynamics, NCED). (right) Niger delta in West Africa. The skeleton network was obtained from *Smart and Moruzzi* [1971] and it is superimposed with a Landsat image. Only links in the networks that connect the delta apex to the shoreline outlets are considered in the connectivity analysis.

of 15) outlets contribute more than 90% of the flux delivered to the coastline. Figures 8b and 8d show the number of outlets receiving fluxes from a given link in the two examined deltas. This plot highlights the relative importance of a link in the delta network: the *hot spot* (red) links affect many outlets while blue links only affect a single outlet. The *hot spots* can be interpreted as “highways of perturbation” since, even if the steady flux in the link is not high, the effect of the perturbation will be experienced by many shoreline outlets in the delta.

The outlet contributing networks for the two examined deltas are shown in Figures 9 and 10 (the colored lines will be discussed in the next section and should be ignored for now). In the Wax Lake delta, most of the outlet contributing networks (18 out of 24, or 67%) have a single path connecting the delta apex to the shoreline outlet. On the contrary, in the Niger delta all the subnetworks have multiple pathways.

In the next section, we present an intuitive approach to quantifying delta vulnerability by assessing the effect of a local flux perturbation to each delta outlet and the delta as a whole. The companion paper [Tejedor *et al.*, 2015] discusses several definitions of the “complexity” of each subnetwork in terms of the number of paths joining the apex to the outlet, number of shared paths with other subnetworks, and number of paths that “leak” fluxes to other subnetworks; this complexity can be used to compare and contrast deltas as well as provide insight into their vulnerability to perturbations.

5. Mapping Vulnerability to Local Flux Perturbations

Having developed a mathematical framework for extracting delta subnetworks and computing their fluxes, we are ready to explore how the fluxes at the shoreline outlets are affected by localized changes in any link of the system. For example, building dikes, dams, and diversions for flood protection or agricultural needs might reduce the flow in some of the channels (vertices), with this reduction propagating downstream according to the overall system connectivity. In extreme cases, some of the system vertices might disappear altogether as channels might be cut off due to lack of sufficient flow to maintain them. We note that in real deltaic systems such alterations would trigger dynamic changes in the network transport, self-organizing some parts of the network in a way that might result in different connectivity. Here we assume, however, that the system connectivity is fixed, and only the fluxes may change due to externally imposed perturbations. In a system science perspective, it is of interest to evaluate how fluxes in every part of the system might change in response to a perturbation in one or more elements of the system. Questions such as what links of the delta network, if altered, might affect most drastically the distribution of fluxes to the coastal outlets, or where an intervention should be imposed to maintain a desired flux to a particular outlet node for land building purposes, are important components of delta management toward sustainability. Here we

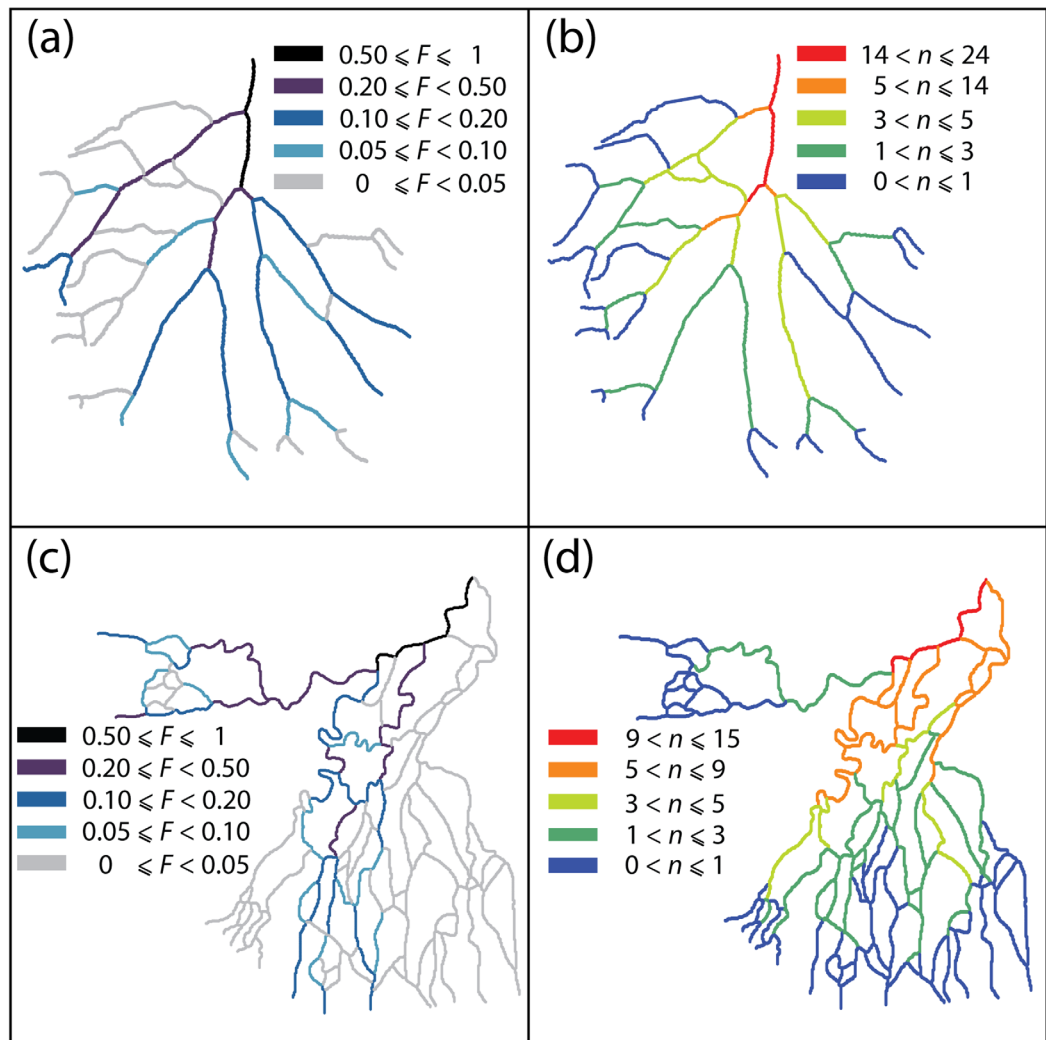


Figure 8. (a and c) Steady state flux, F , and (b and d) number of outlets, n , that link contributes to. (a and b) Wax Lake delta: the distribution of flux among the immediate downstream links is proportional to the channel width. (c and d) Niger delta: the flux is distributed equally among the immediate downstream links. The flux at the apex is normalized to $F = 1$.

demonstrate how we can use the results of sections 2 and 3 to build vulnerability maps that quantify the effect of local flux perturbations to outlet fluxes.

Our framework focuses on delta nodes (graph vertices), while here we prefer to deal with flux changes at links (graph edges). The flux reduction at an edge can be modeled by adding a new artificial outlet z to the vertex v and redistributing the flux F_{uv} between u (flux left) and z (flux lost) so that

$$F_{uv}^{old} = F_{uv}^{new} + F_{zv} = F_{uv}^{old}(1 - \alpha) + F_{uv}^{old}\alpha, \quad 0 \leq \alpha \leq 1.$$

This corresponds to assigning the new weights $w_{zv} = w_{uv}^{old}\alpha$ and $w_{uv}^{new} = w_{uv}^{old}(1 - \alpha)$ to the weighted adjacency matrix W . The coefficient α represents the proportion of the flux lost.

Consider now a link that drains the fraction p , $0 \leq p \leq 1$, of its steady flux to a given outlet. Assume that the steady flux F at this link (see section 3.2) is related to the steady flux O at the outlet as $O/F = B > 0$. The steady flux at the outlet can be then represented as

$$O = \underbrace{Fp}_{\text{Contribution from examined link}} + \underbrace{F(B-p)}_{\text{Contribution from the other links}}. \tag{11}$$

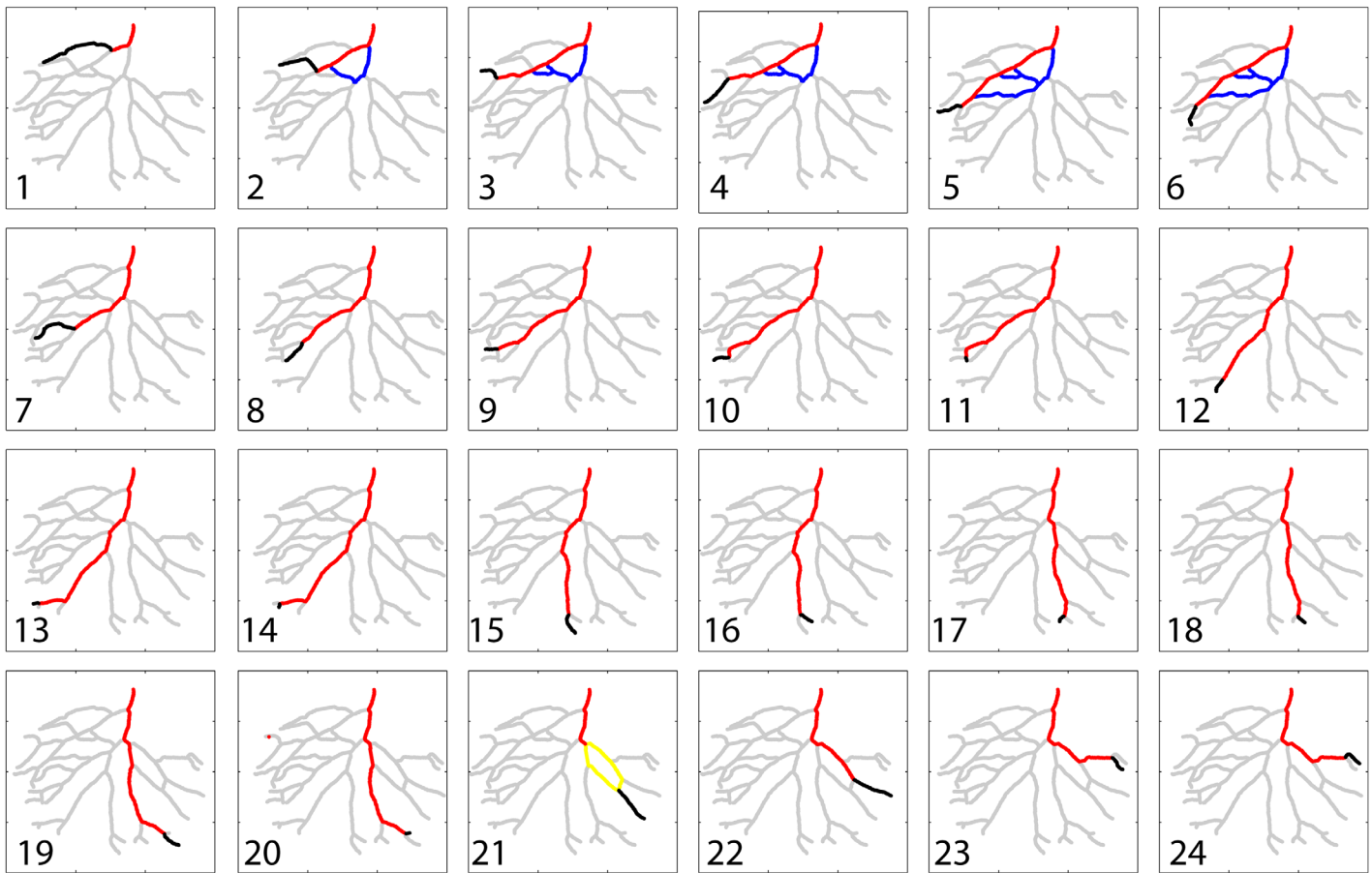


Figure 9. Contributing subnetworks (from apex to outlets) and vulnerability maps for the Wax Lake delta. Each figure highlights the contributing subnetwork for a single outlet (note that all 24 subnetworks shown in the figures were extracted with a single operation as shown in Figure 5 and explained in section 3.3). Shoreline outlets are shown in black. Red, yellow, and blue links represent high ($V_{uv}^i > 0.75$), medium ($0.25 < V_{uv}^i \leq 0.75$), and low ($V_{uv}^i \leq 0.25$) values of the local vulnerability index of equation (13). Notice that if α -reduction is applied to the link (vu), the shoreline outlet will experience a reduction of its steady flux by a factor $\alpha \cdot V_{uv}^i$.

Equation (11) implies that $p \leq B$, which is necessary to ensure that the flux contribution from the links other than the examined one is nonnegative. The α -reduction of the flux at the examined link results in the new flux O^{new} at the outlet:

$$O^{\text{new}} = F(B - \alpha p).$$

The corresponding outlet flux reduction is given by

$$r = 1 - \frac{O^{\text{new}}}{O} = \alpha \frac{p}{B}. \quad (12)$$

We notice that (i) the constraint $p \leq B$, or equivalently $p/B \leq 1$, and hence the outlet flux reduction r cannot exceed the link flux reduction α ; (ii) the perturbed flow at the outlet can be readily obtained from equation (12) *without* recalculating the perturbed steady flow for the entire delta, and (iii) the outlet flux reduction r is always proportional to the link flux reduction α . These useful properties reflect the *linearity* of our transport system. Moreover, from equation (12) we can argue that link (vu) is vulnerable if (i) it drains a large proportion of its steady flux to outlet i ($p \approx 1$), and (ii) it is a significant contributor to the outlet i with respect to other links ($B \approx p$).

To systematically apply these observations to every link (vu) and every outlet i in a delta, we consider quantities p_{uv}^i and B_{uv}^i that are uniquely defined for each pair $\{(vu), i\}$. We now characterize the flux reduction at outlet i with respect to the flux reduction at link (vu) by the *local vulnerability* $V_{uv}^i = p_{uv}^i / B_{uv}^i$. We use the

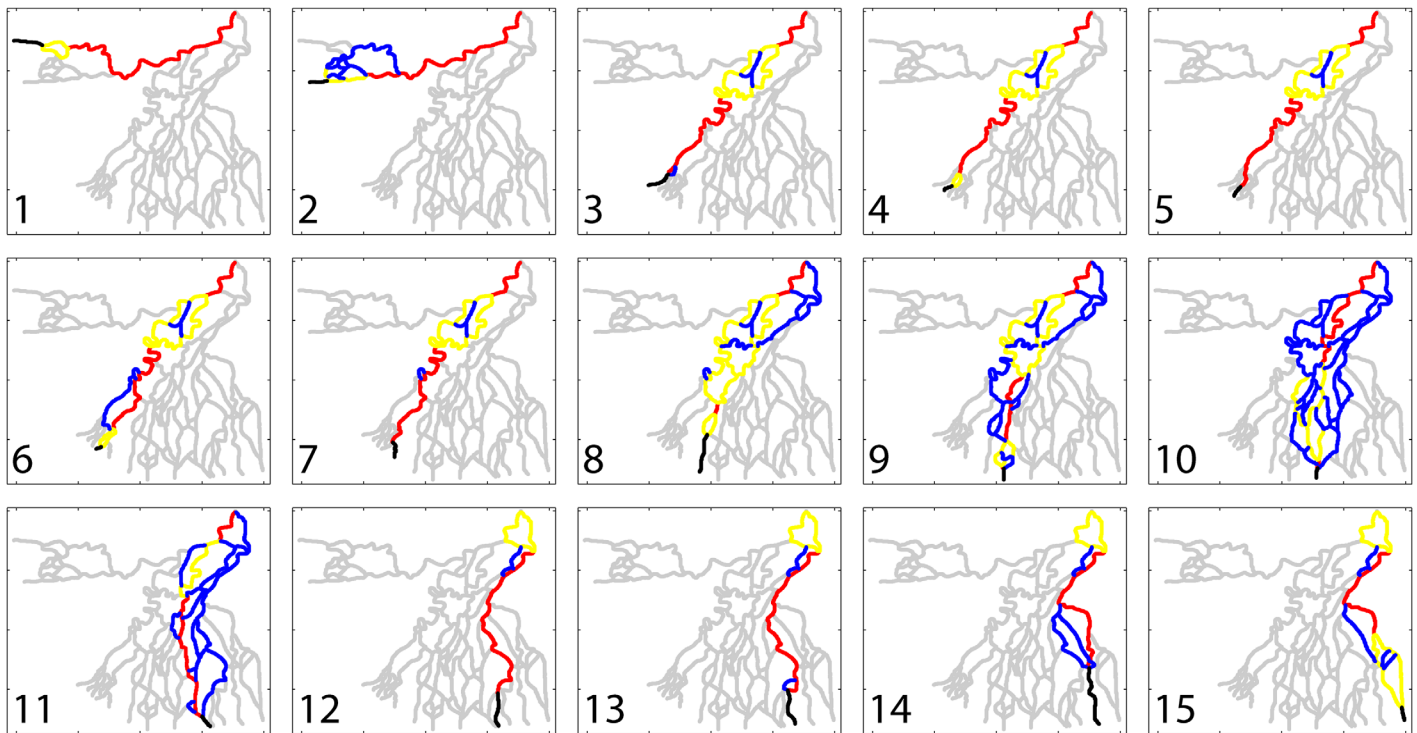


Figure 10. Contributing subnetworks (from apex to outlets) and vulnerability maps for the Niger delta. Each figure highlights the contributing subnetwork for a single outlet. Shoreline outlets are shown in black. Red, yellow, and blue links represent high ($0.75 < V_{uv}^i$), medium ($0.25 < V_{uv}^i \leq 0.75$), and low ($V_{uv}^i \leq 0.25$) values of the local vulnerability index. Notice that if α -reduction is applied to the link (vu), the shoreline outlet will experience a reduction of its steady flux by a factor $\alpha \cdot V_{uv}^i$.

results of section 3.3 to write $p_{uv}^i = \gamma_i(u)$, where $\gamma_i(u)$ is the proportion of the flux at the vertex u that drains to outlet i , so it is also the proportion of the flux at the link (vu) that drains to the outlet i . Furthermore, $B_{uv}^i = F_i / F_{uv}$ by construction. Hence, we express the local vulnerability as

$$V_{uv}^i = \frac{p_{uv}^i}{B_{uv}^i} = \frac{\gamma_i(u) F_{uv}}{F_i} = \frac{\gamma_i(u) F_v w_{uv}}{F_i}, \quad (13)$$

where $\gamma_i(u)$ is described in section 3.3, w_{uv} is the proportion of the flux at a parental vertex v that drains to offspring vertex u , and F_v is the steady flux at vertex v described in section 3.2.

The *global vulnerability* of outlet i is defined as the average of the local vulnerabilities over all links in the subnetwork that drains to outlet i (edges of graph G):

$$V_i = \frac{1}{|E_i|} \sum_{(vu) \in E} V_{uv}^i, \quad (14)$$

where $|E_i|$ denotes the number of links in the subnetwork that drains to outlet i (contributing network for outlet i as described in section 3.3).

As an illustration, we compute here the *local vulnerability* indices at each of the outlets of the Wax Lake and Niger. The results are shown in *vulnerability maps* in Figures 9 and 10 (color code). Each panel illustrates the link vulnerability within the contributing network of a particular outlet. In this analysis, we index the delta nodes in such a way that the outlet indices coincide with the panel numbers. The red, yellow, and blue edges represent high ($V_{uv}^i > 0.75$), medium ($0.25 < V_{uv}^i \leq 0.75$), and low ($V_{uv}^i \leq 0.25$) values of the local vulnerability index.

It is noted that subnetworks dominated by a single path are very vulnerable as a change of flux in that path propagates directly to the outlet. At the same time, subnetworks with many splitting and joining paths are less vulnerable to alterations in individual links of the system. For example, for subnetwork 10 of Niger delta,

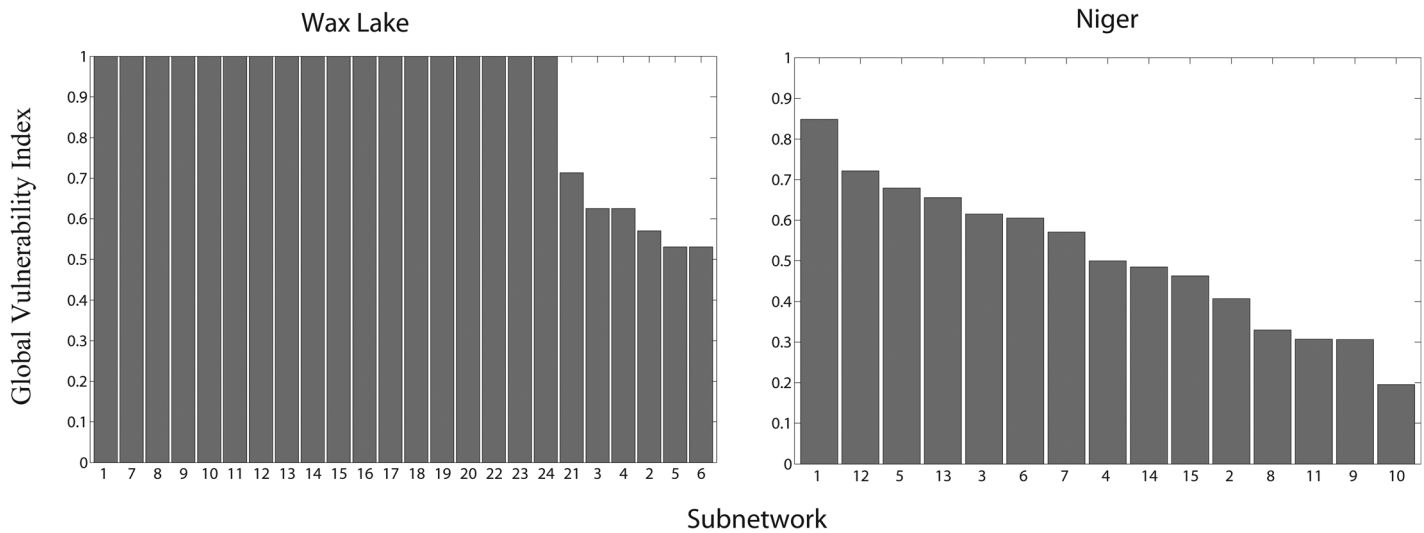


Figure 11. Average vulnerability indices V_i of contributing subnetworks arranged in decreasing order for (left) Wax Lake and (right) Niger deltas (see equation (14) for definition). Each subnetwork is labeled by its outlet number (see Figures 9 and 10). A subnetwork composed of a single path from the apex to the outlet is more vulnerable to a flux change than a subnetwork that includes several interconnected paths.

the *global subnetwork vulnerability* (as defined by equation (14)) is $V_{10} = 0.2$, which means that *on average* if the flux at any of the upstream links that drain to outlet 10 is reduced by a fraction α , the flux to the outlet will be reduced by 0.2α suggesting that upstream alterations (e.g., flux reduction) in those links will not impact considerably the flux at the outlet. This is consistent with the map of Figure 10, where most links in subnetwork 10 are labeled blue. On the contrary, the vulnerability $V_1 = 0.85$ for subnetwork 1 of Niger delta indicates that flux change in a link of this subnetwork will have a large effect on the outlet; e.g., *on average* a reduction by a factor of 0.5 in the link will propagate as a reduction by a factor $0.5 \cdot 0.85 = 0.425$ to the outlet. This is also seen from Figure 10 where most of the links of subnetwork 1 are labeled red.

Figure 11 presents the *global subnetwork vulnerability* V_i for each subnetwork of the Wax Lake and Niger deltas. In general, it is observed that subnetworks with all red links in Figures 9 and 10 (maximum reduction of the outlet flux in response to a link perturbation) are very vulnerable, while subnetworks with mostly blue or yellow links (medium to minimum reduction in the outlet flux in response to a link perturbation) are less vulnerable. Although the examined metrics of response to change (vulnerability maps and vulnerability indices) are very simple, they still present a first cut at seeing the delta as a system where a change in one part affects all other parts as directed by topologic connectivity and flux dynamics. If the interest is not to evaluate the response of perturbations to the outlets but to any other specific nodes of interest, the methodology presented in section 3 can be applied to that purpose.

Subnetwork topology and the potential to exchange flux with nearby subnetworks directly affects the way a change in a link propagates to the outlet. Although here this propagation was computed by an iterative scheme which uses the weighted Laplacian matrix of hundreds of nested downstream pathways for each subnetwork, the question arises as to whether instead of performing these direct computations one can resort to associate (at least qualitatively) vulnerability to metrics that capture the topologic (network) and dynamic (flux exchange) complexity of each subnetwork. Such formal metrics are proposed in the companion paper [Tejedor *et al.*, 2015] and demonstrated in a series of delta channel networks ranging from very simple to very complex ones.

6. Discussion

Although some young deltas, such as the Wax Lake delta, resemble inverted tributary networks, in general, deltaic systems have a much richer topological structure than river networks. Thereby, delta networks are not amenable to the hierarchical branching structure analysis used in river networks which is based on the Hortonian or Tokunaga indexing methods (e.g., for a recent extensive Tokunaga analysis of 400 river

networks, see *Zanardo et al.* [2013]). Horton and Tokunaga indices are difficult to define in deltaic networks due to the existence of loops found at all bifurcating levels from the upstream nodes to the shoreline. To our knowledge, no quantitative tools or frameworks for delta river network analysis exist to date. Our proposed framework aims to fill this gap and offers a powerful machinery to extract all topologically relevant information from delta networks. It is understood that this information forms the basis for any follow-up analysis that tries to relate the mechanistic and physical processes underlying delta formation to the patterns they imprint on the landscapes.

A simple “decomposition” of a delta network system in its distinct subnetworks that connect the apex to the shoreline outlets, reveals that these subnetworks are not independent of each other, i.e., many links are shared among two or more subnetworks (see Figures 8b and 8d, together with Figures 9 and 10). This implies the existence of a “topologic interaction” among the different subnetworks. For instance, in subnetwork 10 of the Niger delta (see Figure 10), there is a big overlap of links with many other subnetworks. Large overlap among delta’s subnetworks might have significant implications for the delta system as a whole: on one hand, a given perturbation will affect a bigger portion of the delta; but on the other hand, the perturbation may be damped because it can be distributed among several subnetworks. Topology is certainly the most important constraint for the flux distribution, but the asymmetric partition of fluxes at each bifurcation also plays a vital role in the dynamic exchange of fluxes among subnetworks, especially for deltas that exhibit preferential flow paths. Thus, the interaction among subnetworks must have two components: topologic and dynamic. The latter takes into account the asymmetry in the flux partition at each bifurcation stemming from the local hydrodynamic and morphodynamic conditions. We have shown in this paper how the proposed framework is able to provide the information required to formulate and start quantifying the complexity that arises from the interaction of subnetworks (topologic and flux-related) and how this complexity affects the ability of the system to propagate external perturbations from its upstream to its downstream links and to the shoreline. A more formal and extensive analysis of the subnetwork topologic and flux interaction in a larger set of deltaic systems is provided in the companion paper [*Tejedor et al.*, 2015].

Defining vulnerability here in terms of the flux change at a shoreline (outlet) node due to flux changes in upstream links, our framework clearly shows that the flux reduction *felt* at an outlet depends on both the fraction of a link’s flux that drains to the outlet, p , and the quotient of the fluxes at the link and the outlet, B . From Figures 9 and 10, it is observed that the existence of multipath connectivity between the apex and the outlet within a subnetwork generally reduces the vulnerability index. This is due to the fact that the flux is able to travel from the apex to the outlet through different paths and therefore a perturbation in a given link will not affect as much the flux at the outlet as in single path subnetworks. These observations support the necessity of a systematic, spatially extended approach to studying the effects of link perturbations on the system as a whole. The framework introduced here allows us to compute easily the spatially extended pairwise characteristics of any upstream link and the examined outlet, p and B . It is important to notice that we have presented here only one scenario of change in the delta, i.e., reduction of flux at a given point of the delta (e.g., due to dam construction); however, the study of vulnerability of other scenarios such as diversion or construction of embankments can be also implemented within the framework. It is hoped that having formal ways to analyze the topology and dynamics of delta networks will open the door to a suite of analyses aiming at understanding how the structure and function of a delta system predisposes itself to certain vulnerabilities, akin, for example, to recent studies in river networks [e.g., *Benda et al.*, 2004; *Carrara et al.*, 2012; *Czuba and Foufoula-Georgiou*, 2014].

We summarize here the main assumptions made in the formulation of our framework that could be relaxed to generalize it or to study a specific system in detail:

1. The steady flux has been computed using channel widths as the only parameter to compute the flux partition in bifurcations (weights in the adjacency matrix). Even though the width is a good surrogate for the flux partition, if a given delta is to be studied in a greater detail, geomorphic and ecohydrologic information (e.g., slope, depth, bed material, vegetation, etc.) can be incorporated in parameterizing the weights to obtain a more realistic flux distribution.
2. We focus on the steady state flux of the delta and consider the long-term impact of flux perturbation in our vulnerability analysis. In order to incorporate specific processes or seasonal forcing, a study of the perturbation time scales and the relaxation times of the delta would be required.

3. The current version of the framework does not incorporate possible dynamic evolution of the delta topology and channel morphology but an extension of the proposed framework to a time-evolving adjacency matrix is possible (see, for example, *Zaliapin et al.* [2010] for a dynamic river network extension concept).
4. The topology of a delta network might be composed of fluvial, tidal, and anthropogenic (artificial) channels that receive fluxes from other sources than simply the river flux at the apex. Although the proposed framework only analyzes the “river component” of the fluxes in the system, other components such as tides and direct rainfall inputs could be integrated by incorporating bidirectionality in some channels and sources of flux located at different parts of the delta.

7. Conclusions

In contrast to the well-studied topology of tributary channel networks (networks that drain to a single outlet), the exploration of the topology of distributary channel networks (networks that originate from a single source and drain to multiple outlets) is still in its infancy. Yet, this topology defines the distribution of network fluxes and dictates how changes in a given part of a network propagate to the rest; it also paves the way to better understand the intricate self-organization of deltaic systems and their vulnerability to external perturbations. Here we presented a rigorous framework based on graph theory within which a river delta, characterized by its channel network, is represented by a directed graph, i.e., a collection of vertices (bifurcations and junctions in the delta) and directed edges (channels in-between vertices, where the direction is given by the flow). All information about the network connectivity can be stored in a sparse *adjacency* matrix that allows us to extract important network topologic information by straightforward algebraic manipulations. In this paper, we have demonstrated how the adjacency matrix can be used to extract subnetworks in the delta system, such as upstream (contributing) and downstream (nourishment) subnetworks for any given network vertex. Of special interest are the subnetworks that connect the apex to the outlet (shoreline) nodes and these subnetworks have been studied here in detail. We have also demonstrated how the proposed framework can be extended to the computation of the steady state flux propagation in the network using the weighted adjacency matrix, where the weights determine the partition of fluxes at bifurcation points (junctions). Finally, we have illustrated how within the proposed framework, a systematic vulnerability analysis can be performed by assessing parts of the network where a change would most significantly affect the downstream or shoreline fluxes. All these results follow directly from the spectral decomposition of the Laplacian (discrete analog of the Laplace operator in a diffusion process derived from the adjacency matrix) for the directed graph that represents the delta network. We note that the proposed framework is not exclusive to deltas; it is directly applicable to any other system that can be modeled by a directed acyclic (no loops from a vertex to itself) graph, such as for example, subsurface pathway networks on hillslopes, groundwater networks of flow, blood vessels and citation networks.

In a companion paper [*Tejedor et al.*, 2015], we apply the approach presented herein to study delta networks in terms of quantifying both their topological complexity and also the complexity that arises from their flux distribution, what we call dynamic complexity. Specifically, we define a suite of metrics that tease out the intricate structure of pathways and flux dynamics. We also present a complementary entropy-based approach, which quantifies “information sharing” among subnetworks via the mutual information (rigid structure) and the conditional entropy (flexibility of paths), shedding a different light into the delta structure and dynamics as well as to the concepts of robustness and vulnerability to perturbations. These metrics are computed for seven deltas of different environmental and morphodynamic settings. In that paper, we set the foundation for a classification of river deltas based on their complexity using both their topologic and dynamic components. We believe that the proposed framework of quantitative analysis of deltaic systems is an essential first step to initiate the conversation on the difficult problem of understanding how structure and form of a delta network can quantitatively reveal physical attributes of the system’s evolution, including its size and age of development and also the physical mechanisms behind its formation.

Notation

$A(G)$	adjacency matrix of graph G .
A^T	transpose of A .
a_{uv}	element of $A(G)$.

B	ratio of the flux at a given link to the flux at the outlet.
C_u	common part of a subnetwork R_u .
d_u^{in}	in-degree of u (number of edges arriving at vertex u).
d_u^{out}	out-degree of u (number of edges leaving vertex u).
D^{in}	in-degree matrix.
D^{out}	out-degree matrix.
D_W^{in}	weighted in-degree matrix.
D_W^{out}	weighted out-degree matrix.
\mathcal{E}	collection of edges.
F_u	steady flux at vertex u .
F_{uv}	steady flow at an edge (vu) , flowing from v to u .
G	graph.
G^{R}	graph reverse of G .
H_u	exclusive part of a subnetwork R_u .
I_N	$N \times N$ identity matrix.
L	directed graph Laplacian.
L^{in}	in-degree directed graph Laplacian.
L^{out}	out-degree directed graph Laplacian.
L_W^{in}	weighted in-degree directed graph Laplacian.
L_W^{out}	weighted out-degree directed graph Laplacian.
O_i	steady flux at the outlet i .
p_{uv}^i	fraction of the link (vu) flux that arrives at the outlet i .
r	flux reduction at a given outlet.
R_u	subnetwork that participates in draining fluxes from the apex to a given vertex u .
\mathcal{V}	collection of vertices.
V_i	global subnetwork vulnerability of outlet i .
V_{uv}^i	local vulnerability; flux reduction at outlet i with respect to the flux reduction at upstream link (vu) .
(vu)	edge from parental vertex v to offspring vertex u .
$W(G)$	weighted adjacency matrix of graph G .
\tilde{W}	cycled version weighted adjacency matrix.
w_{uv}	element of $W(G)$.
\tilde{w}_{uv}	element of \tilde{W} .
α	percent change of flux at a given link.
γ_i	basis of the null-space of the weighted in-degree Laplacian.
$\gamma_i(v)$	element v of the eigenvector γ_i .
Δ	continuous Laplace operator.
λ	eigenvalue.
$\mathbf{0}_N$	$N \times 1$ vector of zeros.

Acknowledgments

This paper precipitated from discussions at the STRESS 4 (Stochastic Transport and Emergent Scaling on the Earth's surface) working group meeting at Lake Tahoe, Nevada on April 2013. This work is part of the International BF-DELTA project on "Catalyzing action towards sustainability of deltaic systems" funded by the Belmont Forum (NSF grant EAR-1342944). It is also a tribute to the "Sustainable Deltas 2015" (SD2015) Initiative endorsed by the International Council of Scientific Unions (ICSU), which aims to increase awareness of delta vulnerability worldwide and foster international collaboration, knowledge, and data exchange for actionable research toward delta sustainability. Partial support by the FESD Delta Dynamics Collaboratory (NSF grant EAR-1135427) and the Water Sustainability and Climate Program (NSF grant EAR-1209402) is gratefully acknowledged. The data in our article can be provided upon request (alej.tejedor@gmail.com). We would also like to thank the Editor Graham Sander, Phairot Chatanantavet, and two anonymous reviewers for their helpful comments that resulted in an improved presentation of our work.

References

- Abam, T. K. S. (2001), Regional hydrological research perspectives in the Niger Delta, *Hydrol. Sci. J.*, *46*, 13–25.
- Adegoke, J. O., M. Fageja, G. James, G. Agbaje, and T. E. Ologunorisa (2010), An assessment of recent changes in the Niger Delta Coastline using satellite imagery, *J. Sustainable Dev.*, *3*(4), 277–296.
- Agavev, R., and P. Chebotarev (2005), On the spectra of nonsymmetric Laplacian matrices, *Linear Algebra Appl.*, *399*, 157–168.
- Anthony, E. J., and N. Gratiot (2012), Coastal engineering and large-scale mangrove destruction in Guyana, South America: An environmental catastrophe in the making?, *Ecol. Eng.*, *47*, 268–273.
- Barrat, A., M. Barthelemy, and A. Vespignani (2008), *Dynamical Processes on Complex Networks*, Cambridge Univ. Press, Cambridge, U. K.
- Bauer, F. (2012), Normalized graph Laplacians for directed graphs, *Linear Algebra Appl.*, *436*, 4193–4222, doi:10.1016/j.laa.2012.01.020.
- Benda, L., K. Andras, D. Miller, and P. Bigelow (2004), Confluence effects in rivers: Interactions of basin scale, network geometry, and disturbance regimes, *Water Resour. Res.*, *40*, W05402, doi:10.1029/2003WR002583.
- Blum, M. D., and H. H. Roberts (2009), Drowning of the Mississippi Delta due to insufficient sediment supply and global sea-level rise, *Nat. Geosci.*, *2*(7), 488–491.
- Bolla Pittaluga, M., R. Repetto, and M. Tubino (2003), Channel bifurcations in braided rivers: Equilibrium configurations and stability, *Water Resour. Res.*, *39*(3), 1046, doi:10.1029/2001WR001112.
- Bucx, T., M. Marchand, A. Makaske, and C. van de Guchte (2010), Comparative assessment of the vulnerability and resilience of 10 deltas—Synthesis report, *Delta Alliance Rep. 1*, Delta Alliance Int., Delft, Netherlands.
- Carrara, F., F. Altermatt, I. Rodriguez-Iturbe, and A. Rinaldo (2012), Dendritic connectivity controls biodiversity patterns in experimental metacommunities, *Proc. Natl. Acad. Sci. U. S. A.*, *109*(15), 5761–5766, doi:10.1073/pnas.1119651109.
- Caughman, J. S., and J. J. P. Veerman (2006), Kernels of directed graph Laplacians, *Electron. J. Comb.*, *13*, R39, 1–8.

- Chen, Z., and D. J. Stanley (1998), Sea-level rise on Eastern China's Yangtze delta, *J. Coastal Res.*, *14*, 360–366.
- Chung, F. K. R. (1997), Spectral graph theory, in *CBMS Regional Conference in Mathematics*, 212 pp., Am. Math. Soc., Providence, R. I.
- Czuba, J. A., and E. Fofoula-Georgiou (2014), A network-based framework for identifying potential synchronizations and amplifications of sediment delivery in river basins, *Water Resour. Res.*, *50*, 3826–3851, doi:10.1002/2013WR014227.
- Edmonds, D., R. Slingerland, J. Best, D. Parsons, and N. Smith (2010), Response of river-dominated delta channel networks to permanent changes in river discharge, *Geophys. Res. Lett.*, *37*, L12404, doi:10.1029/2010GL043269.
- Edmonds, D. A., and R. L. Slingerland (2007), Mechanics of river mouth bar formation: Implications for the morphodynamics of delta distributary networks, *J. Geophys. Res.*, *112*, F02034, doi:10.1029/2006JF000574.
- Edmonds, D. A., and R. L. Slingerland (2010), Significant effect of sediment cohesion on delta morphology, *Nat. Geosci.*, *3*(2), 105–109, doi:10.1038/ngeo730.
- Edmonds, D. A., C. Paola, D. C. J. D. Hoyal, and B. A. Sheets (2011), Quantitative metrics that describe river deltas and their channel networks, *J. Geophys. Res.*, *116*, F04022, doi:10.1029/2010JF001955.
- Euler, L. (1736), Solutio problematis ad geometriam situs pertinentis, *Comment. Acad. Sci. U. Petrop.*, *8*, 128–140. [Reprinted in *Opera Omnia Series Prima* (1766), *7*, 1–10.]
- Fagherazzi, S., A. Bortoluzzi, W. E. Dietrich, A. Adami, S. Lanzoni, M. Marani, and A. Rinaldo (1999), Tidal networks: 1. Automatic network extraction and preliminary scaling features from digital terrain maps, *Water Resour. Res.*, *35*(12), 3891–3904, doi:10.1029/1999WR900236.
- Filip, F., and L. Giosan (2014), Evolution of Chilia lobes of the Danube delta: Reorganization of deltaic processes under cultural pressures, *Anthropocene*, *5*, 65–70, doi:10.1016/j.ancene.2014.07.003.
- Fofoula-Georgiou, E., et al. (2013), A vision for a coordinated international effort on delta sustainability, in *Deltas: Landforms, Ecosystems and Human Activities*, vol. 358, edited by G. Young and G. M. E. Perillo, pp. 3–11, IAHS Publ., Wallingford, U. K.
- Galloway, W. E. (1975), Process framework for describing the morphologic and stratigraphic evolution of deltaic depositional systems, in *Deltas: Models for Exploration*, edited by M. L. Broussard, pp. 87–98, Houston Geol. Soc., Houston, Tex.
- Geleynse, N., V. R. Voller, C. Paola, and V. Ganti (2012), Characterization of river delta shorelines, *Geophys. Res. Lett.*, *39*, L17402, doi:10.1029/2012GL052845.
- Goodbred, S. L., Jr. (2003), Response of the Ganges dispersal system to climate change: A source-to-sink view since the last interstade, *Sediment. Geol.*, *162*, 82–104.
- Goudie, A. S. (2005), The drainage of Africa since the Cretaceous, *Geomorphology*, *67*, 437–456.
- Jerolmack, D. J., and J. B. Swenson (2007), Scaling relationships and evolution of distributary networks on wave-influenced deltas, *Geophys. Res. Lett.*, *34*, L23402, doi:10.1029/2007GL031823.
- Kim, W., A. Dai, T. Muto, and G. Parker (2009a), Delta progradation driven by an advancing sediment source: Coupled theory and experiment describing the evolution of elongated deltas, *Water Resour. Res.*, *45*, W06428, doi:10.1029/2008WR007382.
- Kim, W., D. Mohrig, R. Twilley, C. Paola, and G. Parker (2009b), Is it feasible to build new land in the Mississippi River Delta?, *Eos Trans. AGU*, *90*(42), 373–374, doi:10.1029/2009EO420001.
- Kuenzer, C., S. van Beijma, U. Gessner, and S. Dech (2014), Land surface dynamics and environmental challenges of the Niger Delta, Africa: Remote sensing-based analyses spanning three decades (1986–2013), *Appl. Geogr.*, *53*, 354–368.
- Larsen, L. G., J. W. Harvey, G. B. Noe, and J. P. Crimaldi (2009), Predicting organic floc transport dynamics in shallow aquatic ecosystems: Insights from the field, the laboratory, and numerical modeling, *Water Resour. Res.*, *45*, W01411, doi:10.1029/2008WR007221.
- Liang, M., V. R. Voller, and C. Paola (2015a), A reduced-complexity model for river delta formation: Part 1—Modeling deltas with channel dynamics, *Earth Surf. Dyn.*, *3*, 67–86, doi:10.5194/esurf-3-67-2015.
- Liang, M., N. Geleynse, D. A. Edmonds, and P. Passalacqua (2015b), A reduced-complexity model for river delta formation: Part 2—Assessment of the flow routing scheme, *Earth Surf. Dyn.*, *3*, 87–104, doi:10.5194/esurf-3-87-2015.
- Martin, J., B. Sheets, C. Paola, and D. Hoyal (2009), Influence of steady base-level rise on channel mobility, shoreline migration, and scaling properties of a cohesive experimental delta, *J. Geophys. Res.*, *114*, F03017, doi:10.1029/2008JF001142.
- Newman, M. E. J. (2003), The structure and function of complex networks, *SIAM Rev.*, *45*, 167–256.
- Newman, M. E. J. (2010), *Networks: An Introduction*, 772 pp., Oxford Univ. Press, N. Y.
- Nyman, J. A., and R. D. DeLaune (1999), Four potential impacts of global sea-level rise on coastal marsh stability, *Curr. Top. Wetland Biogeochem.*, *3*, 112–117.
- Paola, C., K. M. Straub, D. C. Mohrig, and L. Reinhardt (2009), The “unreasonable effectiveness” of stratigraphic and geomorphic experiments, *Earth Sci. Rev.*, *97*, 1–43.
- Paola, C., R. R. Twilley, D. A. Edmonds, W. Kim, D. Mohrig, G. Parker, E. Viparelli, and V. R. Voller (2011), Natural Processes in Delta restoration: Application to the Mississippi Delta, *Annu. Rev. Mar. Sci.*, *3*, 67–91, doi:10.1146/annurev-marine-120709-142856.
- Parker, G., C. Paola, K. X. Whipple, and D. C. Mohrig (1998), Alluvial fans formed by channelized fluvial and sheet flow. I. Theory, *J. Hydraul. Eng.*, *124*, 985–995.
- Passalacqua, P., S. Lanzoni, C. Paola, and A. Rinaldo (2013), Geomorphic signatures of deltaic processes and vegetation: The Ganges-Brahmaputra-Jamuna case study, *J. Geophys. Res. Earth Surf.*, *118*, 1838–1849, doi:10.1002/jgrf.20128.
- Rabalais, N. N., R. E. Turner, Q. Dortch, D. Justic, V. J. Bierman, and W. J. Wiseman (2002), Nutrient-enhanced productivity in the northern Gulf of Mexico: Past, present and future, *Hydrobiologia*, *475*, 39–63.
- Reijers, T. A. J. (2011), Stratigraphy and sedimentology of the Niger Delta, *Geologos*, *17*(3), 133–162.
- Rinaldo, A., S. Fagherazzi, S. Lanzoni, M. Marani, and W. E. Dietrich (1999a), Tidal networks: 2. Watershed delineation and comparative network morphology, *Water Resour. Res.*, *35*(12), 3905–3917, doi:10.1029/1999WR900237.
- Rinaldo, A., S. Fagherazzi, S. Lanzoni, M. Marani, and W. E. Dietrich (1999b), Tidal networks: 3. Landscape-forming discharges and studies in empirical geomorphic relationships, *Water Resour. Res.*, *35*(12), 3919–3929, doi:10.1029/1999WR900238.
- Roberts, H. H., R. D. Adams, and R. H. W. Cunningham (1980), Evolution of sand-dominant subaerial phase, Atchafalaya Delta, Louisiana, *AAPG Bull.*, *64*(2), 264–279.
- Roberts, H. H., N. Walker, R. Cunningham, G. P. Kemp, and S. Majersky (1997), Evolution of sedimentary architecture and surface morphology: Atchafalaya and Wax Lake Deltas, Louisiana (1973–1994), *Trans. Gulf Coast Assoc. Geol. Soc.*, *47*(42) 477–484.
- Roberts, H. H., J. M. Coleman, S. J. Bentley, and N. Walker (2003), An embryonic major delta lobe: A new generation of delta studies in the Atchafalaya-Wax Lake Delta system, *Trans. Gulf Coast Assoc. Geol. Soc.*, *53*, 690–703.
- Rodríguez-Iturbe, I., and A. Rinaldo (1997), *Fractal River Basins: Chance and Self-Organization*, 547 pp., Cambridge Univ. Press, Cambridge, U. K.
- Saito, Y., H. Wei, Y. Zhou, A. Nishimura, Y. Sato, and S. Yokota (2000), Delta progradation and chenier formation in the Huanghe (Yellow River) delta, China, *J. Asian Earth Sci.*, *18*, 489–497.

- Sapozhnikov, V. B., and E. Foufoula-Georgiou (1996), Self-affinity in braided rivers, *Water Resour. Res.*, *32*(5), 1429–1439, doi:10.1029/96WR00490.
- Sapozhnikov, V. B., and E. Foufoula-Georgiou (1997), Experimental evidence of dynamic scaling and indications of self-organized criticality in braided rivers, *Water Resour. Res.*, *33*(8), 1983–1991, doi:10.1029/97WR01233.
- Sapozhnikov, V. B., and E. Foufoula-Georgiou (1999), Horizontal and vertical self-organization of braided rivers towards a critical state, *Water Resour. Res.*, *35*(3), 843–851, doi:10.1029/98WR02744.
- Seybold, H., J. S. Andrade Jr., and H. J. Herrmann (2007), Modeling river delta formation, *Proc. Natl. Acad. Sci. U. S. A.*, *104*(43), 16,804–16,809, doi:10.1073/pnas.0705265104.
- Seybold, H. J., P. Molnar, H. M. Singer, J. S. Andrade Jr., H. J. Herrmann, and W. Kinzelbach (2009), Simulation of birdfoot delta formation with application to the Mississippi Delta, *J. Geophys. Res.*, *114*, F03012, doi:10.1029/2009JF001248.
- Shaw, J. B., D. Mohrig, and S. K. Whitman (2013), The morphology and evolution of channels on the Wax Lake Delta, Louisiana, USA, *J. Geophys. Res. Earth Surf.*, *118*, 1562–1584, doi:10.1002/jgrf.20123.
- Short, K. C., and A. J. Staeuble (2004), Outline of geology of Niger delta. *AAPG Bull.*, *51*(5), 761–799.
- Smart, J. S., and V. L. Moruzzi (1971), Quantitative properties of delta channel networks, *Tech. Rep. 3*, 27 pp., IBM Thomas J. Watson Res. Cent., Yorktown, N. Y.
- Syvitski, J. P. M. (2008), Deltas at risk, *Sustainability Sci.*, *3*(1), 23–32, doi:10.1007/s11625-008-0043-3.
- Syvitski, J. P. M., A. J. Kettner, A. Correggiari, and B. W. Nelson (2005), Distributary channels and their impact on sediment dispersal, *Mar. Geol.*, *222–223*, 75–94.
- Syvitski, J. P. M., et al. (2009), Sinking deltas due to human activities, *Nat. Geosci.*, *2*(10), 681–686, doi:10.1038/ngeo629.
- Tejedor, A., A. Longjas, I. Zaliapin, and E. Foufoula-Georgiou (2015), Delta Channel Networks: 2. Metrics of topologic and dynamic complexity for delta comparison, physical inference and vulnerability assessment, *Water Resour. Res.*, doi:10.1002/2014WR016604, in press.
- Vörösmarty, C. J., J. Syvitski, J. Day, A. de Sherbinin, L. Giosan, and C. Paola (2009), Battling to save the world's River Deltas, *Bull. At. Sci.*, *65*(2), 31–43, doi:10.2968/065002005.
- Wolinsky, M., D. A. Edmonds, J. M. Martin, and C. Paola (2010), Delta allometry: Growth laws for river deltas, *Geophys. Res. Lett.*, *37*, L21403, doi:10.1029/2010GL044592.
- Wright, L. D., and J. M. Coleman (1973), Variations in morphology of major river deltas as functions of ocean wave and river discharge regimes, *AAPG Bull.*, *57*(2), 370–398.
- Zaliapin, I., E. Foufoula-Georgiou, and M. Ghil (2010), Transport on river networks: A dynamic tree approach, *J. Geophys. Res.*, *115*, F00A15, doi:10.1029/2009JF001281.
- Zanardo, S., I. Zaliapin, and E. Foufoula-Georgiou (2013), Are American rivers Tokunaga self-similar? New results on fluvial network topology and its climatic dependence, *J. Geophys. Res. Earth Surf.*, *118*, 166–183, doi:10.1002/jgrf.20029.
- Ziv, G., E. Baran, S. Nam, I. Rodríguez-Iturbe, and S. A. Levin (2012), Trading-off fish biodiversity, food security, and hydropower in the Mekong River Basin, *Proc. Natl. Acad. Sci. U. S. A.*, *109*(15), 5609–5614, doi:10.1073/pnas.1201423109.